



Published in final edited form as:

Nutr Cancer. 2013 ; 65(0 1): . doi:10.1080/01635581.2013.785003.

Differential Effect of Grape Seed Extract against Human Non-Small-Cell Lung Cancer Cells: the role of Reactive Oxygen Species and Apoptosis Induction

Alpna Tyagi¹, Komal Raina¹, Subhash Gangar¹, Manjinder Kaur¹, Rajesh Agarwal^{1,2}, and Chapla Agarwal^{1,2,*}

¹Department of Pharmaceutical Sciences, Skaggs School of Pharmacy and Pharmaceutical Sciences, University of Colorado Anschutz Medical Campus, Aurora, CO 80045, USA

²University of Colorado Cancer Center, University of Colorado Anschutz Medical Campus, Aurora, CO 80045, USA

Abstract

Present study examines grape seed extract (GSE) efficacy against a series of Non-small-cell lung cancer (NSCLC) cell lines which differ in their *Kras* and *p53* status to establish GSE potential as a cytotoxic agent against a wide-range of lung cancer cells. GSE suppressed growth and induced apoptotic death in NSCLC cells irrespective of their *k-Ras* status, with more sensitivity towards H460 and H322 (wt *k-Ras*) than A549 and H1299 cells (mutated *k-Ras*). Mechanistic studies in A549 and H460 cells, selected, based on comparative efficacy of GSE at higher and lower doses, respectively, showed that apoptotic death involves cytochrome c release associated caspases 9 and 3 activation, and PARP cleavage, strong phosphorylation of ERK1/2 and JNK1/2, down regulation of cell survival proteins, and up regulated pro-apoptotic Bak expression. Importantly, GSE treatment caused a strong superoxide radical-associated oxidative stress, significantly decreased intracellular reduced glutathione levels, suggesting, for the first-time, the involvement of GSE-caused oxidative stress in its apoptotic inducing activity in these cells. Since GSE is a widely-consumed dietary agent with no known untoward effects, our results support future studies to establish GSE efficacy and usefulness against NSCLC control.

Keywords

Apoptosis; chemoprevention; reactive oxygen species; grape seed extract; lung cancer; natural products

1. Introduction

Lung cancer (LC) is the most frequently diagnosed malignancy and leading cause of cancer-related deaths globally [1]. American Cancer Society, estimates 222,160 new LC cases and 160,340 associated deaths in 2012, in the United States alone [2]. The 5-year survival rate of 16% has only shown a slight improvement over the last 30 years, suggesting that additional approaches and strategies are needed to control this deadly malignancy. In this regard, the major emphasis of several recent studies has been on the identification of natural, non-toxic,

*Address for correspondence: Chapla Agarwal, Department of Pharmaceutical Sciences, Skaggs School of Pharmacy and Pharmaceutical Sciences, University of Colorado Anschutz Medical Campus, 12850 E. Montview Blvd, C238, Room V20-2118, Aurora, CO 80045. Phone: (303) 724-4057, Fax: (303) 724-7266, Chapla.Agarwal@UCDenver.edu.

Conflict of Interest Disclosures: The authors declare that there are no conflicts to disclose.

NIH-PA Author Manuscript

NIH-PA Author Manuscript

NIH-PA Author Manuscript

dietary and/or non-dietary agents for both prevention and intervention of LC [3]. Management of cancer by these agents are anticipated to delay the neoplastic progression to more advanced stages of the disease, that would positively improve the morbidity and survival time in LC patients [4]. Accordingly, several bioactive food components have been identified which account for anti-cancer efficacy of the plants of their origin [5]. One such natural agent is grape seed extract (GSE); which is a complex mixture of procyanidins (polyphenols containing dimers, trimers and other oligomers) and proanthocyanidins (catechin and epicatechin and their gallate derivatives [6]. Previously, we and other have shown GSE efficacy against prostate, colon, breast and other cancers in several cell culture and animal models [7–9].

Constitutive up regulation of oxidative stress contributes to genotypic and phenotypic changes of cancer cells, representing a redox vulnerability which can be targeted selectively by pro-oxidant chemopreventive/therapeutic agents [10]. Interestingly, pro-oxidants induce up regulation of cellular reactive oxygen species (ROS) specifically targeting cancer cells thereby activating signal transduction pathways responsible for cell cycle arrest and/or apoptosis [10], underlining the significance of this mechanism for potential therapeutic targets. The oxidative insult causes DNA, protein and lipid damage, activation of mitogen activated protein kinases (MAPKs) [11], induction of anti-apoptotic proteins (Bcl2, Bcl-x1, survivin and XIAP), and inhibition of pro-apoptotic proteins (Bak, Bad and Bid) [12,13]. The MAPKs family consists of extracellular signal-regulated kinase (ERK1/2), c-Jun N-terminal protein kinase (JNK1/2), and p38 kinase [14]. ERK1/2 is a survival moderator, however sustained ERK1/2 activation might also induce cell death [11]. The activation of JNK1/2 and p38 are generally implicated in the induction of cell death and inflammation after exposure to stress conditions [15]. MAPKs are also known to mediate apoptosis via activation of caspases [16]. Notably, caspases are classically activated by intrinsic and extrinsic pathways involving cytochrome c released from the mitochondria into the cytosol and cell surface death receptors, respectively, eventually leading to caspase 3 activation [12], which cleaves poly (ADP-ribose) polymerase (PARP) leading to cell death via DNA fragmentation [17]. Taken together, we rationalized that generation of oxidative stress in tumor cells by dietary chemopreventive agents could be a useful strategy for the prevention and/or intervention of LC. In the present study, employing a panel of human non-small-cell lung cancer (NSCLC) cell lines, which accounts for 80–85% of the lung cancers, we for the first time evaluated the potential link between the anti-cancer efficacy of GSE, oxidative stress, and apoptotic death.

2. Materials and Methods

2.1. Cell lines and reagents

Human NSCLC A549, H1299 and H460 cells were obtained from American Type Culture Collection (Manassas, VA) and H322 cells were a kind gift from Dr. Daniel Chan (Department of Medicine, Division of Medical Oncology, University of Colorado Denver). RPMI 1640 media and other cell culture materials were from Invitrogen Corporation (Gaithersburg, MD). PD98059 (Cat # 513000, Calbiochem, San Diego CA) and SP600125 (Cat # BML-1305, Enzo Life Sciences, Farmingdale, NY) was used. Primary antibodies for cytochrome c (Cat # 556433) and Bcl-x1 (Cat # 610746) were from BD Pharmingen (San Diego, CA). Antibodies for cleaved caspase 3 (Cat # 9661), cleaved caspase 9 (Cat # 9501), cleaved PARP (Cat # 9541), pERK1/2 (Cat # 9101), pJNK1/2 (Cat # 9251), total ERK1/2 (Cat # 9102), JNK1/2 (Cat # 9252), Bak (Cat # 3814), Bcl2 (Cat #,2876), XIAP (Cat # 2042), and anti-rabbit peroxidase-conjugated secondary antibody (Cat # 7074) were from Cell Signaling (Danvers, MA). Survivin (Cat # NB-500-201) was from Novus Biologicals. α -Tubulin (Cat # sc-5546) was from Santa Cruz Biotechnology (Santa Cruz., CA). N-acetyl-L-cysteine (NAC, Cat # A-9165), dimethylsulfoxide (Cat # 154938) and β -actin (Cat # A2228)

antibody were from Sigma-Aldrich (St. Louis, MO). Annexin V-Vybrant apoptosis kit (Cat # V-13241) was from Molecular Probes (Eugene, Oregon).

2.2. Cell culture and treatments

GSE was a gift from Kikkoman Corporation (Noda City, Japan) and its details about composition and characterization are published earlier.[18,19]. NSCLC cells A549, H1299, H460 and H322 cells were cultured in RPMI 1640 medium containing 10% fetal bovine serum and 1% penicillin-streptomycin under standard culture conditions. At 60–65% confluency, cells were treated for 12–48 h with desired doses of GSE (20–100 $\mu\text{g/ml}$) in DMSO or DMSO alone. Cells were harvested and assessed for viability using the Trypan blue dye exclusion method as published earlier [20]. Unless specified otherwise, the final concentration of DMSO in the culture medium during different treatments did not exceed 0.1% (v/v). In inhibitor experiments, cells were pretreated with 20 mM NAC for 0.5 h, while PD98059 (50 μM) and SP600125 (50 μM) were added for 2 h, prior to the addition of GSE.

Some western blots were multiplexed or stripped and reprobed with different antibodies including those for loading control. As applicable, densitometric analysis of immunoblots was done by Scion Image program (NIH, Bethesda, MD), and densitometric values adjusted to loading controls (β -actin and α -Tubulin) as needed.

2.3. Immunoblotting

At 60–65% confluency, cells were treated as mentioned above and cell lysates were prepared in non-denaturing lysis buffer [10 mM Tris-HCl (pH 7.4), 150 mM NaCl, 1% triton X-100, 1mM EDTA, 1mM EGTA, 0.3 mM phenyl methyl sulfonyl fluoride, 0.2 mM sodium orthovanadate, 0.5% NP40, 5 U/ml aprotinin]. Briefly, media was removed from the culture plates followed by two washings with ice-cold PBS. Subsequently, cells were incubated in lysis buffer for 20 min on ice and collected by scraping. Finally, cell lysates were centrifuged at 4°C for 60 min at 14,000 rpm. Protein concentrations in lysates were determined by Bio-Rad DC protein assay kit (Cat # 500-0111) from Bio-Rad (Hercules, CA). For immunoblotting, total cell lysates were denatured with 2X sample buffer. Samples were subjected to SDS-PAGE on 12 or 16% gel and separated proteins were transferred onto membrane by Western blotting. Membranes were blocked with blocking buffer for 1 h at room temperature. After blocking, the membranes were probed with desired primary antibodies over night at 4°C followed by peroxidase-conjugated appropriate secondary antibody and visualized by ECL detection system (Cat #.RPN2105, GE Healthcare, Buckinghamshire, UK).

2.4. Measurement of superoxide generation

The generation of intracellular ROS was measured using dihydroethidium (DHE) dye at a final concentration of 5 μM . Briefly, cells after treatment with GSE were incubated with DHE for 30 min at 37°C, harvested by trypsinization, washed and resuspended in PBS at 37°C, and analyzed immediately for ethidium fluorescence intensity via flow cytometry and also visualized by using an inverted fluorescence microscope. Microscopic images were taken by AxioCam MrC5 camera at 100X magnification and processed by Axiovision 4.6 (Carl Zeiss microimaging). An increase in ethidium fluorescence intensity is an indicator of increase in cellular superoxide levels.

2.5. Measurement of intracellular reduced glutathione levels

The intracellular reduced glutathione (GSH) levels were measured using ApoGSH Glutathione colorimetric detection kit (Cat # K261-100) procured from BioVision Inc. (Mountain view, CA). Briefly, cells were treated with GSE without or with pre-treatment

with NAC for 30 min. Trypsinized cells were counted and processed to measure intracellular levels of reduced GSH as per manufacturer's instructions provided with the kit. Reduced GSH levels were normalized with total number of cells in control and GSE treated groups, respectively.

2.6. Analysis of cytochrome c release

Cytochrome c release from mitochondria in to cytosol was measured in A549 and H460 cells following desired treatments. Briefly, cells were washed thrice with ice-cold PBS, and then incubated in permeabilization buffer (20 mM HEPES-KOH, pH 7.4, 50 mM KCl, 210 mM mannitol, 70 mM sucrose, 5 mM MgCl₂, 1 mM DTT, 0.1 mM PMSF) containing complete protease inhibitor cocktail (Cat # 11836170001, Roche Molecular Biochemicals, Indianapolis, IN) for 20 min on ice. Cells were homogenized using a pre-chilled Dounce homogenizer for ~40–45 strokes. After a short centrifugation at 1000g for 5 min, the supernatants were again centrifuged at 14,000g for 30 min, and the cytosolic supernatants and mitochondrial pellets were collected. The pellets were washed once with extraction buffer and then finally suspended in mitochondrial lysis buffer (150 mM NaCl, 50 mM Tris-HCl, pH 7.4, 1% NP-40, 0.25% sodium deoxycholate, 1 mM EGTA, and protease inhibitor). Cytosolic fractions were analyzed by immunoblotting.

2.7. Quantitative detection of apoptosis

To quantify GSE-induced apoptotic death of NSCLC cells, cells were plated in 60 mm dishes. At ~50% confluency, cells were treated with GSE for 6–72h. After these treatments, cells were collected by brief trypsinization and washed with PBS twice, and subjected to Annexin V and PI staining using Vybrant Apoptosis Assay Kit 2 following the step-by-step protocol provided by the manufacturer. Stained cells were analyzed by FACS analysis, utilizing the core service of the University of Colorado Cancer Center (Aurora, CO), in order to quantify the apoptotic cells.

2.8. Statistical analysis

Statistical significance of differences between control and treated samples were calculated by one-way ANOVA followed by a Bonferroni's test using SigmaStat version 3.5 software (Jandel Scientific, San Rafael, CA), and *P* values of ≤ 0.05 were considered significant. The data in all cases are representative of at least 3–4 independent studies with reproducible results.

3. Results

3.1. GSE inhibits growth and induces death in human NSCLC cells

First, we evaluated the efficacy of GSE against a panel of human NSCLC cell lines, having wild type *EGFR* gene sequence and different status of *k-Ras* and *p53* genes, namely A549 (mutated *k-Ras* and wt *p53*), H1299 (mutated *k-Ras* and null *p53*), H460 (wt *k-Ras* and wt *p53*) and H322 (wt *k-Ras* and mutated *p53*) cells [21, 22]. GSE at 50, 75 and 100 $\mu\text{g/ml}$ doses caused 41–86% ($P < 0.05$ –0.001), 36–92% ($P < 0.05$ –0.001) and 23–93% ($P < 0.01$ –0.001) growth inhibition of A549 cells after 24, 48 and 72 h treatment, respectively (Fig. 1A). Concomitantly, an increase in A549 dead cell population [35–70% ($P < 0.05$ –0.001), 29–75% ($P < 0.01$ –0.001) and 23–79% ($P < 0.01$ –0.001)] was also observed under the same concentrations and treatment conditions (Fig. 1A). In H1299 cells, similar GSE doses were effective in decreasing the cell growth by 26–85% ($P < 0.001$), 24–61% ($P < 0.05$ –0.001) and 26–74% ($P < 0.001$) at 24, 48 and 72 h, respectively (Fig. 1B), together with significant cell death [20–47% ($P < 0.01$ –0.001, 24 h), 17–34% ($P < 0.01$ –0.001, 48 h) and 16–36% ($P < 0.01$ –0.001, 72 h)] (Fig. 1B). In case of H460 and H322 cells, GSE showed significant effect on

growth inhibition and cell viability at comparatively lower doses (20–50 µg/ml, Fig. 1C & D). Overall, GSE treatment significantly suppressed cell growth and induced cell death in a dose- and a time-dependent manner in all the four cell lines studied. Notably, since these NSCLC cell lines have wild type gene sequence of *EGFR* but differ genetically in the status of critical gene such as *k-Ras* [21], which is part of the major causes of chemotherapy resistance/failure, our findings showing strong GSE inhibitory effects in all of these cell lines have significant translational implications in NSCLC management.

3.2. GSE induces apoptotic death in human NSCLC cells

GSE treatment induced strong apoptotic death ranging from 26–44% ($P<0.001$), 24–48% ($P<0.001$) and 11–38% ($P<0.001$) in A549 cells at 24, 48 and 72 h, respectively (Fig. 2A); however, similar GSE treatments caused only 2–22% ($P<0.001$), 2–16% ($P<0.001$) and 2–14% ($P<0.001$) apoptotic death in H1299 cells (Fig. 2B). Unlike A549 and H1299 cells, a much lower GSE concentration was effective in inducing apoptosis for H460 and H322 cell lines based on their cell death effects with GSE in Fig 1. Based on these results showing strong apoptotic effect of GSE in a panel of human NSCLC cell lines, we selected two cell lines, A549 (mutated *k-Ras*) and H460 (wt *k-Ras*), representing GSE inhibitory effect at high and low concentrations, respectively, for detailed mechanistic studies.

3.3. GSE activates various attributes of apoptosis in NSCLC A549 and H460 cells

GSE caused a strong and mostly dose-dependent phosphorylation of ERK1/2 and JNK1/2 without any noticeable change in their total protein levels in both the cell lines (Fig. 3A); however, it did not affect phospho/total p38 levels (data not shown). Furthermore, we observed that GSE treatment strongly decreases the protein levels of Bcl-xL, Bcl2, XIAP and survivin, while Bak levels increase at lower doses in A549 (Fig. 3B, left panel). Similar results were observed in H460 cells; however Bcl-xL protein expression was not changed after GSE treatment (Fig. 3B, right panel).

Based on the results shown in Fig. 3A and 3B, next we assessed the involvement of both extrinsic and intrinsic pathways in GSE-caused apoptotic death of these NSCLC cell lines. GSE did not activate caspase 8 in either cell lines (data not shown), suggesting a lack of involvement of extrinsic apoptosis pathway. However, GSE treatment caused a significant release of cytochrome c in the cytosol (Fig. 3C), as well as cleavage of caspases 9 and 3, and PARP in both A549 and H460 cell lines (Fig. 3D), suggesting an overall involvement of intrinsic pathway in these apoptotic effects of GSE.

3.4. GSE increases superoxide generation in NSCLC A549 and H460 cells

Epifluorescence studies in A549 cells indicated mild ethidium fluorescence staining [23] in untreated control cells, indicating a basal level of oxidative stress in these cancerous cells; however, GSE treatment caused a robust increase (2 folds, $P<0.001$) within 30 min, which slowly declined thereafter (Fig. 4A). In H460 cells, red nuclear ethidium fluorescence was almost absent in the control H460 cells. However, the GSE treated cells showed bright red nuclear ethidium fluorescence indicative of ROS superoxide radical generation. FACS analysis revealed a time dependant increase in ethidium fluorescence intensity in GSE treated cells (Fig. 4B). Further, FACS analysis also revealed a significant time dependant increase in the percentage of cells positive for ethidium fluorescence indicating the potential of GSE to cause oxidative stress in most of the cells; a 5 fold increase ($P<0.001$) in ROS generation was detected within 1 h and maximal enhancement (6 folds, $P<0.001$) was detected by 3 h which remained sustained even till 12 h (data not shown). The generated ROS was specifically of superoxide radical type; no H₂O₂ could be detected by staining experiments with DCFH₂-DA dye. These results verified that GSE resulted in superoxide radical associated oxidative stress in both A549 and H460 cells.

3.5. GSE decreases GSH levels in NSCLC A549 and H460 cells

Reduced GSH is an important intracellular anti-oxidant involved in maintaining intracellular reduction-oxidation balance [10], and therefore, GSH levels were next examined in GSE treated cells. Fig. 5A and 5B (left panel) clearly show that the level of GSH was significantly reduced by 82% [$P < 0.001$ (A549 cells)] and 60% [$P < 0.001$ (H460)] after GSE treatment following 12 and 6 h, respectively. Further, to determine whether anti-oxidant, NAC, would be able to reduce the GSE induced oxidative stress, NSCLC cells were pre-treated with NAC (20 mM) for 30 min before the addition of GSE for 12 and 6 h in A549 and H460 cells, respectively. Results indicated that indeed NAC was able to significantly recover GSE-caused decrease in the GSH level in both A549 and H460 cells (~40%, $P < 0.001$ for both, Fig. 5A and 5B, right panel). These results suggest that GSE produces intracellular ROS which might be responsible for the reduction in the reduced GSH levels, and this additionally suggests that oxidative stress is generated by GSE which eventually leads to apoptotic death, which was studied next.

3.6. GSE induces ERK1/2 and JNK1/2 activation, cytochrome c release and apoptosis via ROS-dependent mechanism

To finally relate ROS generation, ERK1/2 and JNK1/2 activation, cytochrome c release and apoptosis, cells were treated with NAC for 30 min or PD98059 (MAPK kinase inhibitor) or SP600125 (JNK1/2 inhibitor) for 2 h earlier to GSE treatment and analyzed for ERK1/2 and JNK1/2 activation, cytochrome c release and apoptosis. Pre-treatment with NAC caused a strong inhibition of GSE-caused ERK1/2 activation in both cell lines without altering the total protein levels; however GSE-caused JNK1/2 activation was unaltered by NAC pre-treatment in A549 cells, while H460 cells showed strong inhibition of JNK1/2 activation (Fig. 6A and 6B, left panel). Furthermore, NAC pre-treatment followed by GSE exposure significantly reversed apoptotic cell death ($P < 0.001$, for both) induced by GSE alone in A549 and H460 cells, respectively (Fig. 6A and B, right panel). These results suggested that indeed ROS plays an important role in inducing the activation of ERK1/2 and JNK1/2 followed by apoptosis in A549 and H460 cells after the GSE treatment. We therefore also assessed whether GSE-caused ERK1/2 and JNK1/2 activation directly plays any role in its apoptotic effects, by using selective chemical inhibitors. When cells were pre-treated for 2 h with PD98059, GSE-caused ERK1/2 activation was inhibited in both A549 and H460 cells (Fig. 6A and B, left panel), together with a partial, though significant, reversal in GSE-induced apoptotic cell death in both A549 and H460 cell lines (Fig. 6A and B, right panel). In other studies, SP600125 pre-treatment did not reverse GSE-induced JNK1/2 activation (data not shown) or apoptosis in A549 cells (Fig. 6A, right panel), but H460 cells showed a significant reversal of JNK1/2 activation and apoptosis following SP600125 pre-treatment (Fig. 6B). The concentration of SP600125 used in the present study may be limiting for A549 cell line, and probably is responsible for failure to block the JNK1/2 activation by GSE in this cell line. Together these inhibitor studies suggested that whereas GSE-caused oxidative stress plays a major role in ERK1/2 phosphorylation, the activated ERK1/2 plays only a moderate role in the apoptotic death in both cell lines, and that GSE-caused oxidative stress induces apoptotic death by another mechanism. More interestingly, similar conclusion could be drawn for GSE-caused oxidative stress and JNK1/2 activation and their roles in apoptosis induction in H460 cells; on the other hand the observed JNK1/2 activation by GSE was independent of the involvement of GSE-caused oxidative stress and played no role in apoptotic death of A549 cells. These observations suggested that more studies are needed in future to identify additional pathways involved in apoptotic effects of GSE in these NSCLC cell lines.

The role of GSE-caused oxidative stress was also assessed in the activation of intrinsic apoptotic pathway by assessing cytochrome c release in both A549 and H460 cell lines

which were pre-treated with NAC followed by GSE. The cytochrome c release in to the cytosol was completely blocked in both the cell lines by NAC pre-treatment (Fig. 6C), suggesting that indeed ROS plays a major role in the disruption of mitochondrial membrane potential and subsequent release of cytochrome c into the cytosol.

4. Discussion

Chronic tobacco exposure is the main cause of *k-Ras* mutations in the lung and its mutations contribute to the 30% lung adenocarcinoma [24]. Presence of *k-Ras* mutations in LC patients is considered as a poor prognostic factor. Interestingly, in the present study, GSE induces apoptotic cell death in NSCLC cells irrespective of their *k-Ras* status. Most importantly, in the present study we observed that cells (H460 and H322) harboring wt *k-Ras* mutations are more sensitive to GSE treatment than cells (A549 and H1299) harboring mutated *k-Ras*. Together, these results indicate that most of the human NSCLC tumors will be sensitive to GSE, signifying strong translational potential of our findings.

In line with earlier studies in different cancer models, [17,25], in the present study also, GSE induces apoptosis in NSCLC cells. However, in depth understanding of the factors that regulate apoptosis in GSE treated cancer cells are yet to be accomplished. Thus, in the present study, we explored to uncover the mechanism involved for inducing the apoptosis in GSE treated NSCLC cells.

Uncontrolled oxidative stress describes a state of the cell in which the cellular antioxidant guard mechanisms are inadequate to counteract ROS, or undue ROS is produced, or both. It is a well-known fact that large amount of oxidative stress causes severe damage to cellular components such as lipids, proteins, sugar and nucleic acid-bases, which compromises cellular viability or vital functions [26,27]. Further, damage by oxidative stress to any cellular constituent, if unrestricted, causes development of several human diseases such as cancer and cardiovascular disease etc. [28,29]. However, oxidative stress may also exert diverse cytotoxic and pro-apoptotic functions that would hamper tumorigenicity and malignant progression by altering signal transduction pathways culminating into cell cycle arrest and/or apoptosis, depending on the extent/severity of oxidative stress [10]. Most of the cancer cells show inherent constitutive oxidative stress that maintains tumor growth and protects these cells representing a redox vulnerability which can be targeted selectively by pro-oxidant chemopreventive/ therapeutic agents [30,31].

Accordingly, our detailed study revealed that GSE induced oxidative stress via superoxide formation and depletion of total intracellular GSH levels in NSCLC cells. Decreased total intracellular GSH levels were reversed by NAC pre-treatment prior to GSE exposure in these cells and the results advocate that GSE produces intracellular oxidative stress which might be responsible for the reduced GSH levels. Importantly, these observations are in line with previous published study, where reduced intracellular GSH level were reported to be an important regulator of death and survival of cancer cells [10].

Recent literature reveals that cells not only adapt to harmful oxidative stress utilizing intracellular antioxidant defense system, but eventually educate themselves to use ROS in their favor. These toxic species can contribute essentially to the maintenance of cellular homeostasis by targeting key signaling molecules, such as MAPKs and NF- κ B by altering kinases/ phosphatases regulating their activity [32], cell survival proteins expression and cytochrome c release [33]. In the present study, we found that GSE effectively induced ERK1/2 and JNK1/2 activation. Further, we also observed that GSE caused oxidative stress is the major player for the activation of ERK1/2 and JNK1/2 activation and apoptosis, however, activation of ERK1/2 and JNK1/2 is partially responsible for the induction of

apoptosis in A549 and H460 cells. Though further studies are needed to define the role of oxidative stress induced ERK1/2 and JNK1/2 activation in GSE treated NSCLC cells; our completed studies suggest the important role of oxidative stress in the pro-apoptotic efficacy of GSE.

However, the oxidative stress induced activation of ERK1/2 and JNK1/2, and cytochrome c release in the cytosol are not the only events responsible for the induction of apoptosis in GSE treated A549 and H460 cells; the results also suggest the involvement of additional pathways which might contribute to the induction of apoptosis after GSE treatment. Further, there are collective evidences that suggest cell survival proteins (Bcl-xl, Bcl2, XIAP and survivin) are strong apoptosis inhibitors, the expression of which is increased in cancer cells as compared to normal cells [34,35]. Therefore, modulation of the apoptotic proteins by GSE, results in a significant induction of apoptosis in A549 and H460 cells. Interestingly, GSE induced oxidative stress was not found to play any role in this modulation, thus some other alternative pathways may be involved in their inhibition after GSE treatment. The results of this study indicate that GSE induces apoptosis via at least two major pathways involving oxidative stress and inhibition of cell survival proteins expression. Based on these findings, more studies are needed in future to evaluate both anti-cancer and chemopreventive efficacy of GSE in appropriate pre-clinical LC models to establish its potential usefulness against human lung cancer.

Acknowledgments

This work was supported by the R01 grants CA91883 from the National Cancer Institute and AT003623 from the National Center for Complementary and Alternative Medicine.

Abbreviations

DHE	dihydroethidium
ERK1/2	extracellular signal-regulated kinase
GSE	grape seed extract
GSH	glutathione
JNK1/2	c-Jun N-terminal protein kinase
MAPKs	mitogen activated protein kinases
LC	Lung Cancer
NSCLC	non-small-cell lung cancer
NAC	N-acetyl-L-cysteine
PARP	poly (ADP-ribosyl) polymerase
ROS	reactive oxygen species
IAPs	inhibitor of apoptosis proteins
GSH	glutathione

References

1. Goeckenjan G. Lung cancer - historical development, current status, future prospects. *Pneumologie*. 2010; 64:555–559. [PubMed: 20827638]
2. American Cancer Society. *Cancer Facts and Figures*. 2012.

3. Amin AR, Wang D, Zhang H, Peng S, Shin HJ, et al. Enhanced anti-tumor activity by the combination of natural compounds, (–)-epigallocatechin-3-gallate and luteolin: potential role of p53. *J Biol Chem*. 2010; 285:34557–34565. [PubMed: 20826787]
4. Naithani R, Huma LC, Moriarty RM, McCormick DL, Mehta RG. Comprehensive review of cancer chemopreventive agents evaluated in experimental carcinogenesis models and clinical trials. *Curr Med Chem*. 2008; 15:1044–1071. [PubMed: 18473802]
5. Tan HL, Thomas-Ahner JM, Grainger EM, Wan L, Francis DM, et al. Tomato-based food products for prostate cancer prevention: what have we learned? *Cancer Metastasis Rev*. 2010; 29:553–568. [PubMed: 20803054]
6. Kaur M, Agarwal C, Agarwal R. Anticancer and cancer chemopreventive potential of grape seed extract and other grape-based products. *J Nutr*. 2009; 139:1806S–1812S. [PubMed: 19640973]
7. Raina K, Singh RP, Agarwal R, Agarwal C. Oral grape seed extract inhibits prostate tumor growth and progression in TRAMP mice. *Cancer Res*. 2007; 67:5976–5982. [PubMed: 17575168]
8. Velmurugan B, Singh RP, Kaul N, Agarwal R, Agarwal C. Dietary feeding of grape seed extract prevents intestinal tumorigenesis in APC^{min/+} mice. *Neoplasia*. 2010; 12:95–102. [PubMed: 20072658]
9. Song X, Siriwardhana N, Rathore K, Lin D, Wang HC. Grape seed proanthocyanidin suppression of breast cell carcinogenesis induced by chronic exposure to combined 4-(methylnitrosamino)-1-(3-pyridyl)-1-butanone and benzo[a]pyrene. *Mol Carcinog*. 2010; 49:450–463. [PubMed: 20146248]
10. Wondrak GT. Redox-directed cancer therapeutics: molecular mechanisms and opportunities. *Antioxid Redox Signal*. 2009; 11:3013–3069. [PubMed: 19496700]
11. Sung B, Ravindran J, Prasad S, Pandey MK, Aggarwal BB. Gossypol induces death receptor-5 through activation of ROS-ERK-chop pathway and sensitizes colon cancer cells to trail. *J Biol Chem*. 2010; 285:35418–35427. [PubMed: 20837473]
12. Danial NN. BCL-2 family proteins: critical checkpoints of apoptotic cell death. *Clin Cancer Res*. 2007; 13:7254–7263. [PubMed: 18094405]
13. LaCasse EC, Mahoney DJ, Cheung HH, Plenchette S, Baird S, et al. IAP-targeted therapies for cancer. *Oncogene*. 2008; 27:6252–6275. [PubMed: 18931692]
14. Kralova J, Sheely JI, Liss AS, Bose HR Jr. ERK and JNK activation is essential for oncogenic transformation by v-Rel. *Oncogene*. 2010; 29:6267–6279. [PubMed: 20802521]
15. Gu M, Raina K, Agarwal C, Agarwal R. Inositol hexaphosphate downregulates both constitutive and ligand-induced mitogenic and cell survival signaling, and causes caspase-mediated apoptotic death of human prostate carcinoma PC-3 cells. *Mol Carcinog*. 2010; 49:1–12. [PubMed: 19544333]
16. Hu H, Jiang C, Li G, Lu J. PKB/AKT and ERK regulation of caspase-mediated apoptosis by methylseleninic acid in LNCaP prostate cancer cells. *Carcinogenesis*. 2005; 26:1374–1381. [PubMed: 15845651]
17. Kaur M, Agarwal R, Agarwal C. Grape seed extract induces anoikis and caspase-mediated apoptosis in human prostate carcinoma LNCaP cells: possible role of ataxia telangiectasia mutated-p53 activation. *Mol Cancer Ther*. 2006; 5:1265–1274. [PubMed: 16731759]
18. Veluri R, Singh RP, Liu Z, Thompson JA, Agarwal R, et al. Fractionation of grape seed extract and identification of gallic acid as one of the major active constituents causing growth inhibition and apoptotic death of DU145 human prostate carcinoma cells. *Carcinogenesis*. 2006; 27:1445–1453. [PubMed: 16474170]
19. Chou SC, Kaur M, Thompson JA, Agarwal R, Agarwal C. Influence of gallate esterification on the activity of procyanidin B2 in androgen-dependent human prostate carcinoma LNCaP cells. *Pharm Res*. 2010; 27:619–627. [PubMed: 20162340]
20. Tyagi A, Gu M, Takahata T, Frederick B, Agarwal C, et al. Resveratrol selectively induces DNA Damage, independent of Smad4 expression, in its efficacy against human head and neck squamous cell carcinoma. *Clin Cancer Res*. 2011; 17:5402–5411. [PubMed: 21705453]
21. Ling YH, Aracil M, Jimeno J, Perez-Soler R, Zou Y. Molecular pharmacodynamics of PM02734 (elisidepsin) as single agent and in combination with erlotinib; synergistic activity in human non-small cell lung cancer cell lines and xenograft models. *Eur J Cancer*. 2009; 45:1855–1864. [PubMed: 19346126]

22. Mateen S, Tyagi A, Agarwal C, Singh RP, Agarwal R. Silibinin inhibits human nonsmall cell lung cancer cell growth through cell-cycle arrest by modulating expression and function of key cell-cycle regulators. *Mol Carcinog.* 2010; 49:247–258. [PubMed: 19908243]
23. Li GX, Hu H, Jiang C, Schuster T, Lu J. Differential involvement of reactive oxygen species in apoptosis induced by two classes of selenium compounds in human prostate cancer cells. *Int J Cancer.* 2007; 120:2034–2043. [PubMed: 17230520]
24. Riely GJ, Marks J, Pao W. KRAS mutations in non-small cell lung cancer. *Proc Am Thorac Soc.* 2009; 6:201–205. [PubMed: 19349489]
25. Tyagi A, Agarwal R, Agarwal C. Grape seed extract inhibits EGF-induced and constitutively active mitogenic signaling but activates JNK in human prostate carcinoma DU145 cells: possible role in antiproliferation and apoptosis. *Oncogene.* 2003; 22:1302–1316. [PubMed: 12618755]
26. Dalle-Donne I, Rossi R, Colombo R, Giustarini D, Milzani A. Biomarkers of oxidative damage in human disease. *Clin Chem.* 2006; 52:601–623. [PubMed: 16484333]
27. Packer L, Cadenas E. Oxidants and antioxidants revisited. New concepts of oxidative stress. *Free Radic Res.* 2007; 41:951–952. [PubMed: 17729110]
28. Gibson SB. A matter of balance between life and death: Targeting reactive oxygen species (ROS)-induced autophagy for cancer therapy. *Autophagy.* 2010; 6:835–837. [PubMed: 20818163]
29. Essick EE, Sam F. Oxidative stress and autophagy in cardiac disease, neurological disorders, aging and cancer. *Oxid Med Cell Longev.* 2010; 3:168–177. [PubMed: 20716941]
30. Xiao D, Powolny AA, Moura MB, Kelley EE, Bommareddy A, et al. Phenethyl isothiocyanate inhibits oxidative phosphorylation to trigger reactive oxygen species-mediated death of human prostate cancer cells. *J Biol Chem.* 2010; 285:26558–26569. [PubMed: 20571029]
31. Mackenzie GG, Sun Y, Huang L, Xie G, Ouyang N, et al. Phospho-Sulindac (OXT-328), a Novel Sulindac Derivative, Is Safe and Effective in Colon Cancer Prevention in Mice. *Gastroenterology.* 2010; 139:1320–1322. [PubMed: 20600034]
32. Tarrega C, Nunes-Xavier C, Cejudo-Marin R, Martin-Perez J, Pulido R. Studying the regulation of MAP Kinase by MAP Kinase phosphatases in vitro and in cell systems. *Methods Mol Biol.* 2010; 661:305–321. [PubMed: 20811991]
33. Woo JH, Kim YH, Choi YJ, Kim DG, Lee KS, et al. Molecular mechanisms of curcumin-induced cytotoxicity: induction of apoptosis through generation of reactive oxygen species, down-regulation of Bcl-XL and IAP, the release of cytochrome c and inhibition of Akt. *Carcinogenesis.* 2003; 24:1199–1208. [PubMed: 12807727]
34. Okamoto K, Okamoto I, Okamoto W, Tanaka K, Takezawa K, et al. Role of survivin in EGFR inhibitor-induced apoptosis in non-small cell lung cancers positive for EGFR mutations. *Cancer Res.* 2010; 70:10402–10410. [PubMed: 21159653]
35. Kumar P, Coltas IK, Kumar B, Chepeha DB, Bradford CR, et al. Bcl-2 protects endothelial cells against gamma-radiation via a Raf-MEK-ERK-survivin signaling pathway that is independent of cytochrome c release. *Cancer Res.* 2007; 67:1193–1202. [PubMed: 17283155]

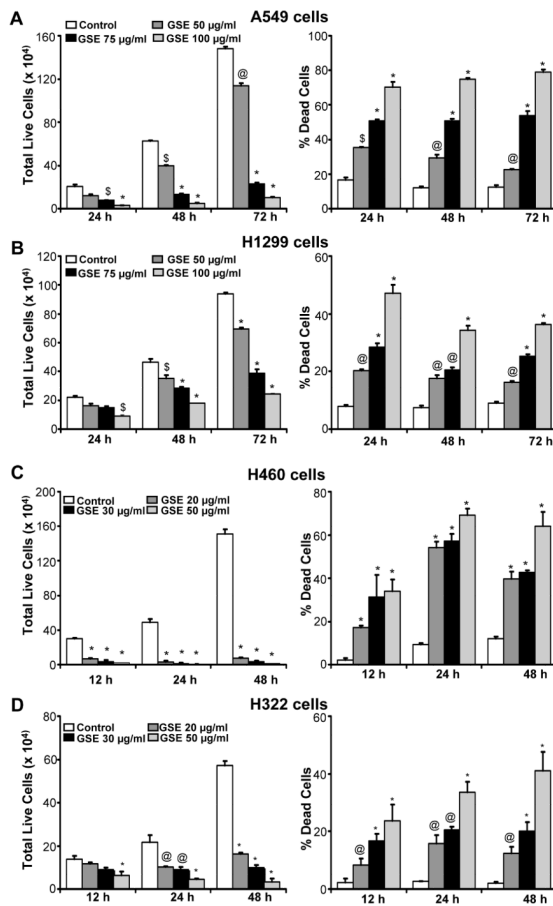


Figure 1. GSE inhibits growth and induces death of human NSCLC cells
 GSE inhibits growth and induces death in A) A549, B) H1299, C) H460 and D) H322 cells, in both dose- and time- dependent manner. Cells (1.05×10^5) were plated in 60 mm dishes, treated with DMSO (control) or different concentrations of GSE, and after 12, 24, 48 or 72 h, cells were harvested and counted as detailed in Materials and Methods section. \$, $P < 0.05$; @, $P < 0.01$; *, $P < 0.001$ for differences with control group. GSE, grape seed extract.

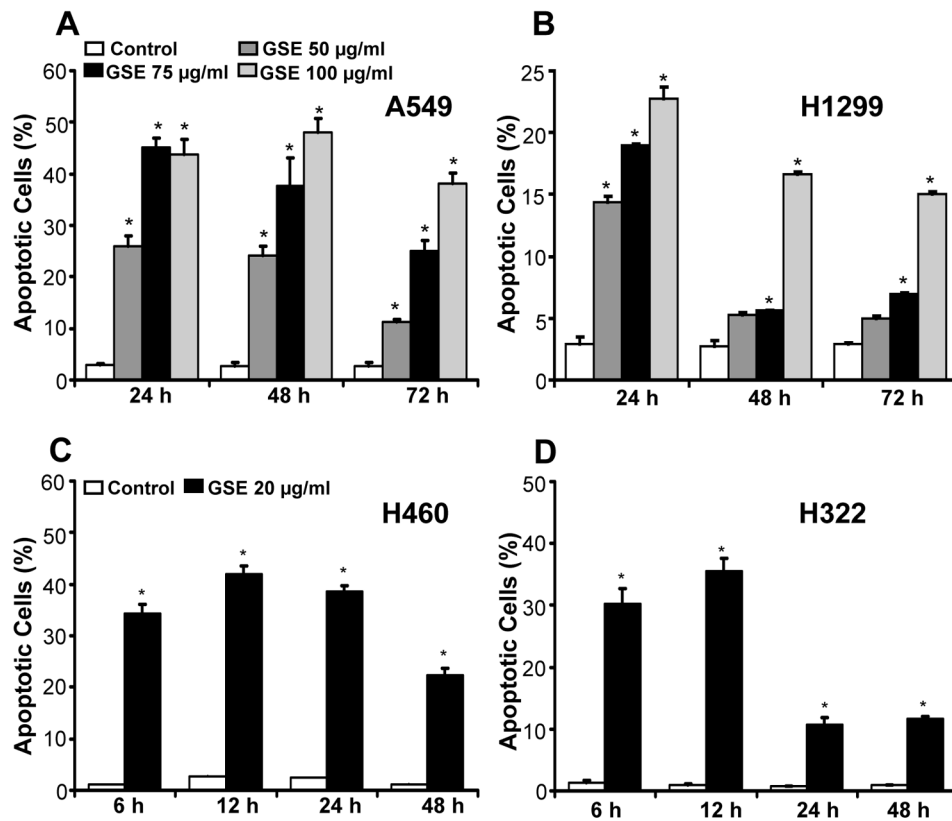


Figure 2. GSE induces apoptotic death of human NSCLC cells

GSE induces apoptotic death in A) A549, B) H1299, C) H460 and D) H322 cells. Cells were treated with DMSO (control) or GSE for the mentioned time and dose as detailed Materials and Methods section. At the conclusion of the experiment, cells were collected by trypsinization, washed with PBS, and subsequently stained with Annexin V- PI. Stained cells were processed for FACS analysis. *, $P < 0.001$ for differences with control group; GSE, grape seed extract.

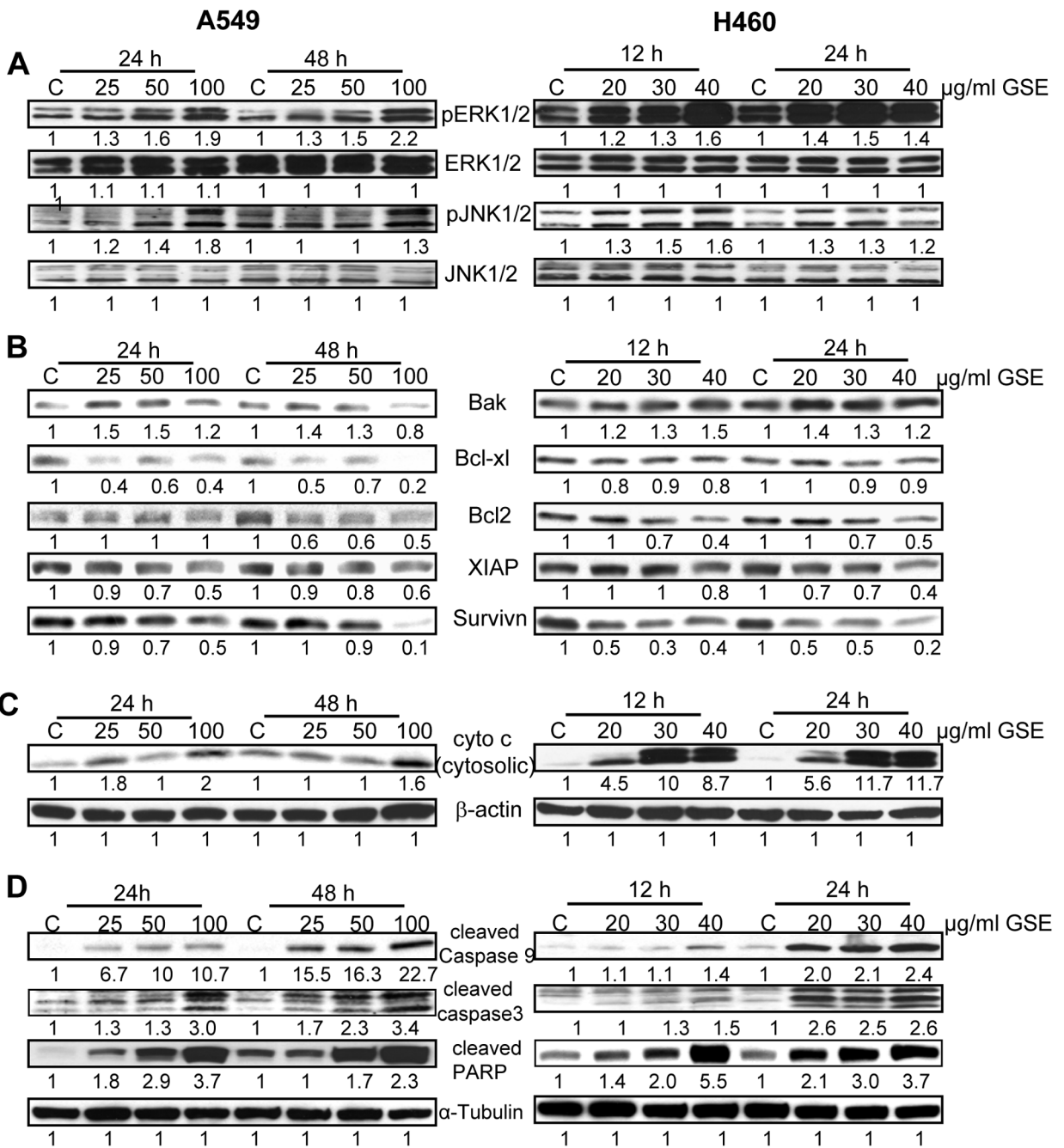


Figure 3. GSE induces various attributes of apoptosis in NSCLC A549 and H460 cells
 A549 and H460 cells were cultured as described in Materials and Methods section, and treated with either DMSO alone (control) or varying concentrations of GSE. At the end of the treatments, total cell lysates were prepared and subjected to SDS-PAGE followed by Western immunoblotting. Membranes were probed with desired primary antibodies followed by peroxidase-conjugated appropriate secondary antibodies and visualized by ECL detection system. The densitometric data presented below the bands are ‘fold change’ compared to respective DMSO control, after normalization with respective loading control (α -Tubulin and β -actin). C, Control; GSE, grape seed extract.

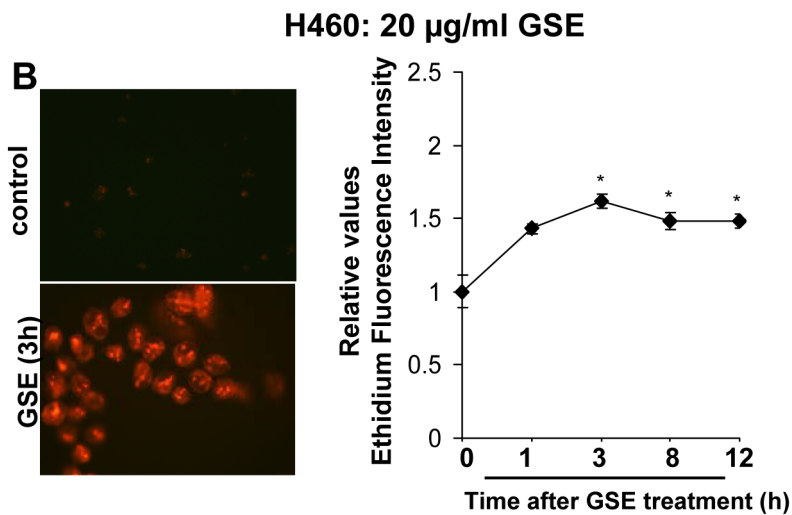
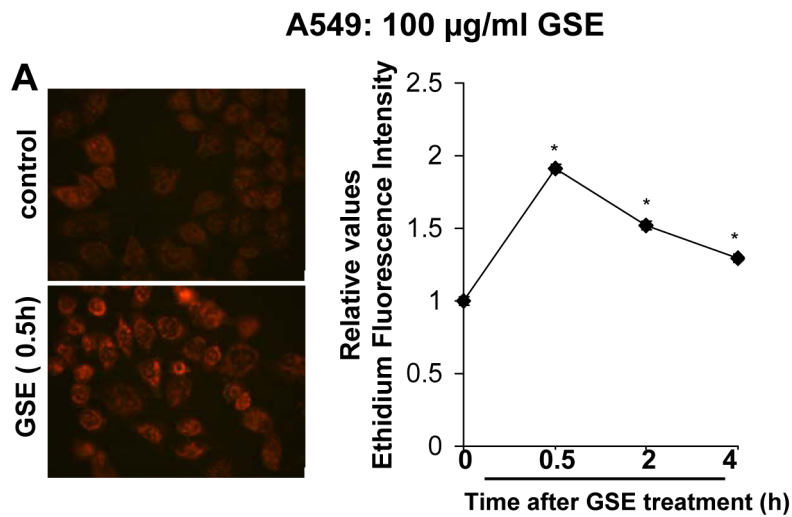


Figure 4. GSE increases superoxide generation in NSCLC A549 and H460 cells

A) A549 and B) H460 cells after treatment with GSE were incubated with DHE for 30 min at 37°C, harvested by trypsinization, washed and re-suspended in PBS at 37°C, and analyzed immediately for ethidium fluorescence intensity via flow cytometry and also visualized by using an inverted fluorescence microscope. In case of shorter GSE exposures, cells were incubated with GSE and DHE together. Superoxide generation in NSCLC cells was indicated by increased ethidium fluorescence after DHE staining. GSE, grape seed extract; *, $P < 0.001$ for differences with control group.

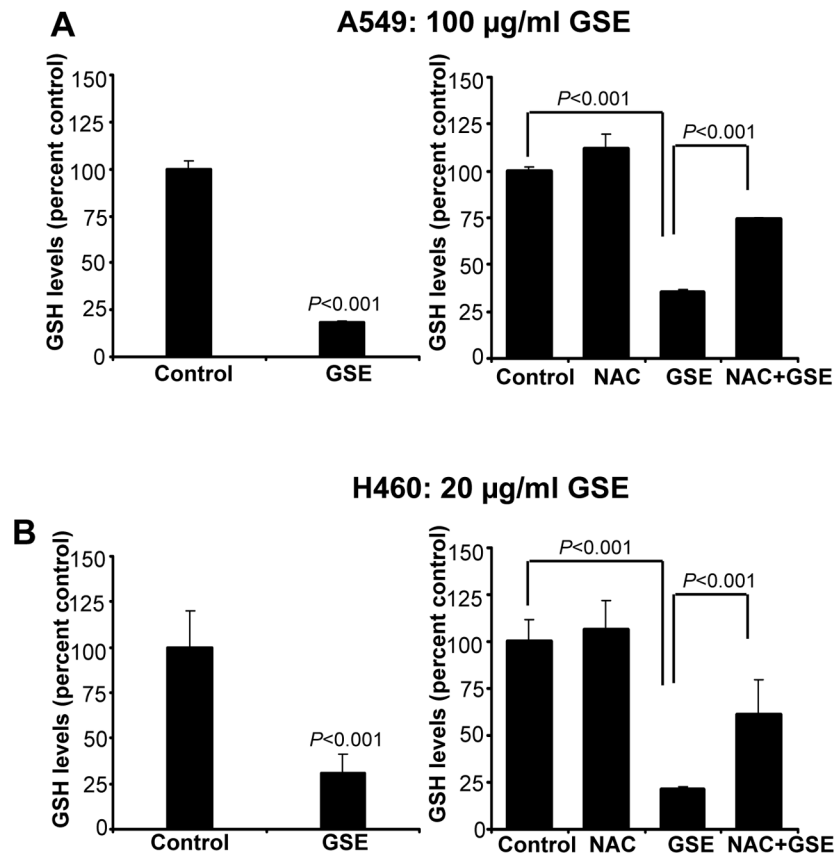


Figure 5. GSE causes depletion of intracellular GSH levels

Treatment of A) A549 and B) H460 cells with 100 $\mu\text{g/ml}$ and 20 $\mu\text{g/ml}$ GSE, respectively, resulted in significant decrease in the intracellular levels of reduced GSH as compared to control cells. Pre-treatment of NAC (20 mM) for 30 min prior the GSE exposure in A549 for 12 h and in H460 for 6 h reversed the GSE inhibited GSH level. The intracellular reduced glutathione levels were measured using ApoGSH Glutathione colorimetric detection kit. Briefly, at the end of the experiments, trypsinized cells were counted and processed to assess intracellular levels of reduced GSH. Reduced GSH levels were normalized with total number of cells in control and GSE treated groups, respectively. NAC, N-acetyl-L-cysteine; GSE, grape seed extract; GSH, glutathione

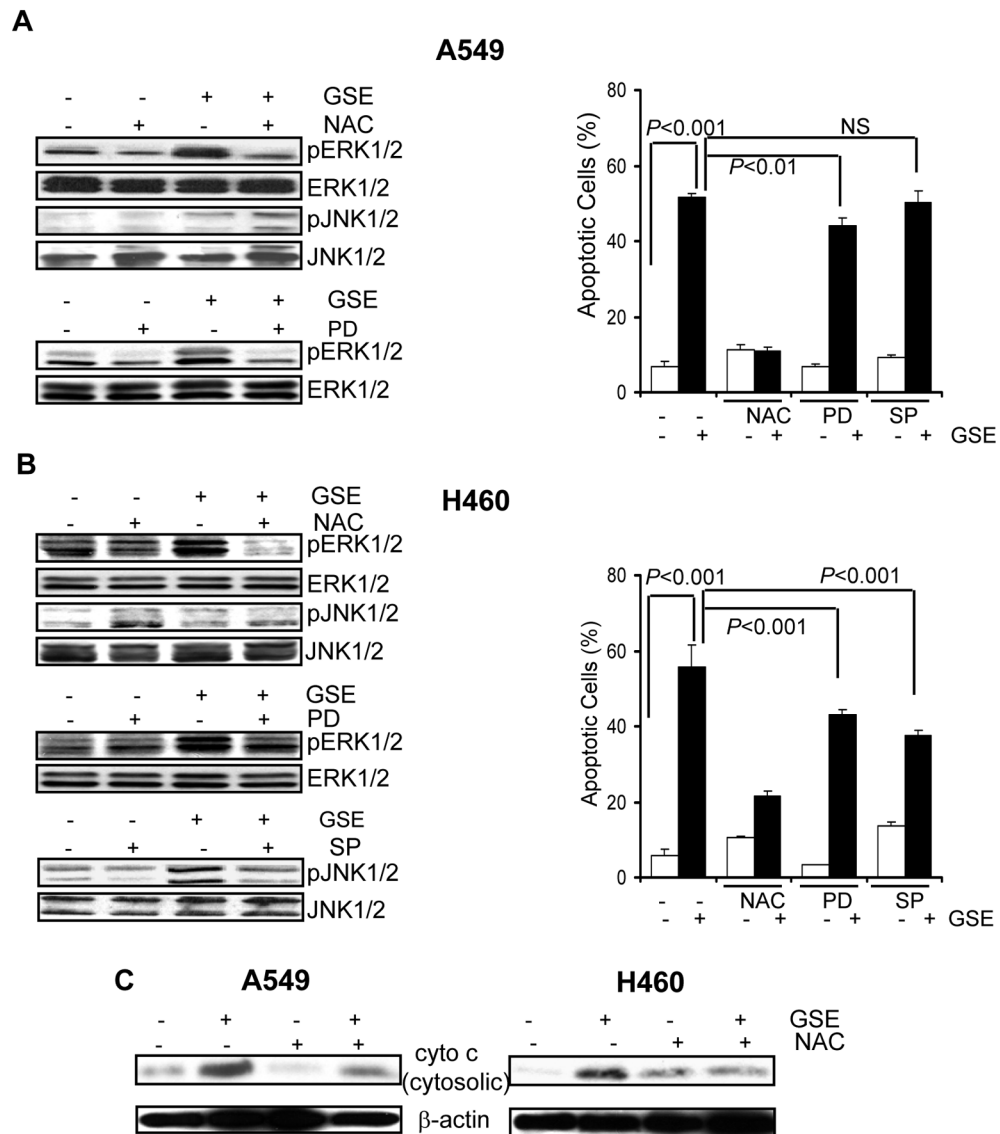


Figure 6. GSE induces ERK1/2 and JNK1/2 activation, cytochrome c release and apoptosis via ROS-dependent mechanism

A) A549 and B) H460 cells were pre-treated with either NAC (30 min)/PD98059/SP600125 (2 h) prior the addition of GSE in A549 (100 $\mu\text{g}/\text{ml}$, 24 h) and H460 (20 $\mu\text{g}/\text{ml}$, 12h) cells. After these treatments, lysates were prepared for Western blot analysis as described in Materials and Methods section. Further, after similar treatments, cells were collected by brief trypsinization and washed with PBS twice, and subjected to Annexin V - PI staining using Vybrant Apoptosis Assay Kit2 following the protocol as described in 'Materials and Methods' section. After staining, FACS analysis was performed for the quantification of the apoptotic cells. C) Pre-treatment with NAC (30 min) prior the addition of the GSE in A549 (100 $\mu\text{g}/\text{ml}$, 24 h) and H460 (20 $\mu\text{g}/\text{ml}$, 12 h) cells, and at the conclusion of the experiment mitochondrial and cytosolic lysates were prepared and subjected to SDS-PAGE followed by Western immunoblotting for detection of cytochrome c (cyto c) levels as described in the 'Materials and Methods' section. GSE, grape seed extract; NAC, N-acetyl-L- cysteine; PD, PD98059, SP, SP600125; NS, non significant.